

MOULD FILLING SIMULATION USING FINITE ELEMENTS

R. CODINA¹, U. SCHÄFER² AND E. OÑATE¹

¹*Escola Tècnica Superior d'Enginyers de Camins, Canals i Ports, Universitat Politècnica de Catalunya, Gran Capità s/n,
Mòdul C1, 08034 Barcelona, Spain*

²*Institut für Statik und Dynamic der Luft- und Raumfahrtkonstruktionen, Pfaffenwaldring 27, 7000 Stuttgart 70,
Germany*

ABSTRACT

In this paper we consider several aspects related to the application of the pseudo-concentration technique to the simulation of mould filling processes. We discuss, in particular, the smoothing of the front when finite elements with interior nodes are employed and the evacuation of air through the introduction of temporary free wall nodes. The basic numerical techniques to solve the incompressible Navier–Stokes equations are also briefly described. The main features of the numerical model are the use of div-stable velocity–pressure interpolations with discontinuous pressures, the elimination of the pressure via an iterative penalty formulation, the use of the SUPG approach to deal with convection-dominated problems and the temporal integration using the generalized trapezoidal rule. At the end of the paper we present some numerical results obtained for a two-dimensional test problem showing the ability of the method to capture complicated flow patterns.

KEY WORDS Div-stability Penalty Upwinding Pseudo-concentration

INTRODUCTION

Mould filling is the first stage of the casting process, an ancient metal forming technique. It starts with the pouring of a molten metal into a mould until it is filled and it is concluded when the solid nature of the metal is restored. The complete numerical simulation of these processes involves modelling of mould filling, prediction of thermal stresses in a solidifying material and micro–macro modelling in order to predict material micro-structure. Besides the inherent difficulty in modelling all these physical phenomena, another problem arises because of the identification of material properties, for which delicate experiments are needed.

The main difficulty when simulating the flow of a molten metal in a mould is the modelling of free surfaces. Most of the numerical approaches to this problem have been limited to simple geometries, due to the high computational cost of this simulation and that numerical models have been mainly based on finite difference techniques. Because of the available computer potential, it has become possible to deal with more complicated geometries for which finite-element models are especially well suited. The representation of feeders, gating systems, risers and the overall mould geometry does not offer any difficulty when using finite elements. Proper evaluation of the position of the melt front during the transient analysis is the most important problem.

The model that we shall use here to track the free surface of the fluid is based upon the pseudo-concentration technique, also known as *volume of fluid* (VOF) method⁸. This technique employs a fixed mesh, the element of which may be filled partially or fully. The version of this method we shall use is due to Thompson^{12,13}. The basic idea is to introduce a scalar function which is advected according to the velocity field obtained from the solution of the Navier–Stokes equations. This function is defined on the whole computational domain. A certain isovalue contour is used to define the front of the *real* fluid. The unfilled region is assumed to be occupied by a fictitious material whose physical properties are such that its motion does not affect the dynamical behaviour of the fluid under consideration. To fix ideas, we shall consider that this fictitious material is air.

The pseudo-concentration technique has been used by several authors to follow free surfaces of creeping flows and viscoplastic flows in the context of metal forming processes, such as extrusion, forging and rolling. See, e.g., References 1, 7, 13. For applications of this method to mould filling, see References 6, 11.

This paper is organized as follows. The statement of the problem is presented in the next section where the basic idea of the pseudo-concentration technique is also explained. The numerical strategy is then described, considering first the discretization in space, based on a Petrov–Galerkin formulation. An iterative penalty technique is used to eliminate the pressure from the momentum equations. The next two sections address some problems arising in the application of the pseudo-concentration technique to mould filling. Finally a practical numerical example is presented.

THE NAVIER–STOKES EQUATIONS WITH A MOVING FREE SURFACE

In this section we shall consider the general problem for an incompressible fluid in laminar regime and taking into account thermal effects, as well as the existence of a free surface within the domain Ω to be occupied by the fluid.

The mechanical and thermal equations describing the problem are:

$$\begin{aligned} \rho \left[\frac{\partial \mathbf{u}}{\partial t} + (\mathbf{u} \cdot \nabla) \mathbf{u} \right] - 2\nabla \cdot [\mu \varepsilon(\mathbf{u})] + \nabla p &= \rho \mathbf{f} \\ \nabla \cdot \mathbf{u} &= 0 \\ \rho c_p \left[\frac{\partial \vartheta}{\partial t} + (\mathbf{u} \cdot \nabla) \vartheta \right] - \nabla \cdot (k \nabla \vartheta) &= Q \end{aligned} \quad (1)$$

to be solved in $\Omega \times (0, T)$, where $[0, T]$ is the time interval to be considered. In Equations (1), \mathbf{u} denotes the velocity field, p the pressure, ϑ the temperature, ρ the density, μ the dynamical viscosity, which may depend on the invariants of the symmetrical part of the velocity gradient $\varepsilon(\mathbf{u})$, \mathbf{f} the body forces, c_p the specific heat at constant pressure, k the thermal conduction coefficient and Q the heat sources.

Let $\boldsymbol{\sigma}$ be the stress tensor and \mathbf{n} the unit outward normal to the boundary $\partial\Omega$. Denoting by an overbar prescribed values, the boundary conditions for the velocity and the temperature to be considered here are:

$$\begin{aligned} \mathbf{u} &= \bar{\mathbf{u}} && \text{on } \Gamma_{du} \\ \mathbf{n} \cdot \boldsymbol{\sigma} &= \bar{\mathbf{t}} && \text{on } \Gamma_{nu} \\ \mathbf{u} \cdot \mathbf{n} = \bar{u}_n, \mathbf{n} \cdot \boldsymbol{\sigma} \cdot \mathbf{g}_1 = \bar{t}_1, \mathbf{n} \cdot \boldsymbol{\sigma} \cdot \mathbf{g}_2 = \bar{t}_2 &&& \text{on } \Gamma_{mu} \\ \vartheta &= \bar{\vartheta} && \text{on } \Gamma_{dt} \\ -k \mathbf{n} \cdot \nabla \vartheta &= \bar{\varphi} && \text{on } \Gamma_{nt} \end{aligned} \quad (2)$$

for $t \in (0, T)$. The boundary $\partial\Omega$ has been considered split into three sets of disjoint components Γ_{du} , Γ_{nu} and Γ_{mu} , the latter being the part of the boundary where mixed conditions are prescribed: the normal velocity and the tangent stresses. Vectors \mathbf{g}_1 and \mathbf{g}_2 (for the three-dimensional case) span the space tangent to Γ_{mu} . Also, Γ_{dt} and Γ_{nt} are the two disjoint components of $\partial\Omega$ where Dirichlet and Neumann boundary conditions for the temperature are prescribed, respectively. Initial conditions have to be appended to problems defined by (1)–(2).

Concerning the tracking of the free surface, the basic idea of the pseudo-concentration technique is to define a scalar function, say $\psi(\mathbf{x})$, over the computational domain Ω in such a manner that its value at a certain point $\mathbf{x} \in \Omega$ indicates the presence or absence of fluid. This function may be considered as a fictitious fluid property. For instance, we may assign the value 1 to regions where the fluid has already entered and the value 0 to air-filled regions. The position of the fluid front will be defined by the isovalue contour $\psi(\mathbf{x}) = \psi_c$, where $\psi_c \in [0, 1]$ is a critical value defined *a priori*. We usually take $\psi_c = 0.5$. This value is immaterial if ψ is a true step function, but is needed in the finite element discretization and for the smoothing to be described later.

The conservation of the pseudo-concentration (assumed to be sufficiently smooth) in any control volume $V_i \subset \Omega$ which is moving with the divergence-free velocity field \mathbf{u} leads to:

$$\frac{\partial \psi}{\partial t} + (\mathbf{u} \cdot \nabla) \psi = 0 \quad \text{in } \Omega, t \in (0, T)$$

This equation is hyperbolic and therefore boundary conditions for ψ have to be specified at the inflow boundary, defined as:

$$\Gamma_{\text{inf}} := \{\mathbf{x} \in \partial\Omega \mid \mathbf{u} \cdot \mathbf{n} < 0\}$$

The definition of the position of the fluid front will be given by the physical properties. Let π be any of these, i.e., density (ρ), viscosity (μ), specific heat (c_p) or conduction coefficient (k). We will have that

$$\pi(\mathbf{x}, t) = \begin{cases} \pi_{\text{fluid}}(\mathbf{x}, t) & \text{if } \mathbf{x} \in \Omega_f \\ \pi_{\text{air}} & \text{if } \mathbf{x} \in \Omega \setminus \Omega_f \end{cases} \quad (3)$$

where

$$\Omega_f := \{\mathbf{x} \in \Omega \mid \psi(\mathbf{x}, t) \geq \psi_c\}$$

and the pseudo-concentration function ψ is the solution of the following problem:

$$\begin{aligned} \frac{\partial \psi}{\partial t} + (\mathbf{u} \cdot \nabla) \psi &= 0 & \text{in } \Omega, t \in (0, T) \\ \psi &= \bar{\psi} & \text{on } \Gamma_{\text{inf}}, t \in (0, T) \\ \psi(\mathbf{x}, 0) &= \psi_0(\mathbf{x}) & \text{in } \Omega \end{aligned} \quad (4)$$

The initial condition ψ_0 is chosen in order to define the initial position of the fluid to be analyzed. The boundary condition $\bar{\psi}$ determines whether fluid enters or not through a certain point of the inflow boundary. If it does, a value $\bar{\psi} \geq \psi_c$ is to be prescribed (for example, $\bar{\psi} = 1$); else, $\bar{\psi} < \psi_c$. We will come back to this point later.

This is the formulation of the pseudo-concentration method. In (3), the property π for the fluid-filled region is allowed to depend on the unknowns of the problem, whereas it has been considered constant for the air, i.e., for the fictitious fluid. Observe that, since the physical properties will be discontinuous across the fluid front, the differential equations (1) will not exactly describe the conservation of momentum, mass and energy, since the jump of these properties has been ignored. Observe also, that since the fluid under consideration and the air are treated simultaneously, no boundary conditions at the interface between them are needed. For example, thermal boundary layers, usually dealt with by imposing a heat flux proportional

to the temperature jump, will be approximated depending on the mesh size and on the ability of the numerical formulation to capture high gradients. Nonlinear radiation conditions and other physical effects, such as surface tension at the fluid front have to be neglected using the pseudo-concentration technique.

NUMERICAL MODEL

Space discretization and SUPG method

After choosing a suitable finite element partition $\{\Omega^e\}$ of the domain Ω , with index e ranging from 1 to the number of elements N_{el} , the standard Galerkin method applied to (1) and the transport equation (4) will lead to an initial value problem of the form:

$$\mathbf{M}_v \cdot \frac{d}{dt} \mathbf{U} + \mathbf{K}_c(\mathbf{U}) \cdot \mathbf{U} + \mathbf{K}_d(\mu) \cdot \mathbf{U} - \mathbf{G} \cdot \mathbf{P} = \mathbf{F}_v \quad (5)$$

$$\mathbf{G}^T \cdot \mathbf{U} = \mathbf{0} \quad (6)$$

$$\mathbf{M}_t \cdot \frac{d}{dt} \Theta + \mathbf{H}_c(\mathbf{U}) \cdot \Theta + \mathbf{H}_d \cdot \Theta = \mathbf{F}_t \quad (7)$$

$$\mathbf{M}_f \cdot \frac{d}{dt} \Psi + \mathbf{J}(\mathbf{U}) \cdot \Psi = \mathbf{F}_f \quad (8)$$

The following notation has been employed: capital letters \mathbf{U} , \mathbf{P} , Θ and Ψ denote the vectors of nodal unknowns of the corresponding lower case variables (velocity, pressure, temperature and pseudo-concentration, respectively); subscript v refers to the momentum equation (for the velocity), t to the temperature equation and f to the pseudo-concentration equation; \mathbf{M} (with the appropriate subscript) denotes the standard mass (or Gramm) matrix; \mathbf{F} the discrete force terms; \mathbf{K}_c and \mathbf{K}_d are the convective and diffusive (viscous) matrices for the Navier–Stokes equations and \mathbf{H}_c , \mathbf{H}_d their analogues for the energy balance equation; \mathbf{G} is the discrete gradient matrix; and \mathbf{J} is the matrix coming from the convective term of the pseudo-concentration equation. It is understood that the force terms account for both the Dirichlet and the Neumann-type boundary conditions. The dependence of all the arrays on the velocity has been explicitly indicated, as well as the dependence of \mathbf{K}_d on the viscosity.

In what follows, we shall assume thermally uncoupled flow, so that the temperature equation may be solved once the solution \mathbf{U} , \mathbf{P} for the Navier–Stokes equations is found.

Let us discuss first the choice of the finite element spaces for the velocity and the pressure. It is well known that due to the zero-divergence restriction (6) these spaces have to satisfy the Babuška–Brezzi (BB) stability condition (often referred to as div-stability, for the problem currently considered). Moreover, we shall use a penalty method (see below) and it is therefore desirable to use discontinuous pressure interpolations, since this allows to eliminate the pressure at the element level in terms of the velocity unknowns. After substitution of the resulting expression in the momentum equation one ends up with a problem only involving velocities, and not pressures, as unknowns. For the examples presented, we have used the Q_2/P_1 element, which is constructed using a continuous biquadratic interpolation for the velocity components (in 2-D) and piecewise discontinuous linear pressures. See, e.g., Reference 14 for further discussion about the available velocity-pressure pairs.

Concerning the finite element spaces for the temperature and the pseudo-concentration, we have used for both fields the same interpolation as for the velocity components.

When the convective term in a transport equation becomes important the standard Galerkin formulation fails and numerical oscillations occur. Upwind techniques must be devised in order to overcome this problem. Here, we shall briefly describe the streamline-upwind/Petrov–Galerkin

(SUPG) formulation² employed in our calculations. Consider, for instance, the momentum equations. The basic idea of the SUPG method is to perturb the standard test functions of the Galerkin approach, say \mathbf{v}_h , and to consider instead $\mathbf{v}_h + \zeta_h$, where ζ_h is given by:

$$\zeta_h = \tau^e (\mathbf{u}^e \cdot \nabla) \mathbf{v}_h \tag{9}$$

This perturbation is discontinuous across interelement boundaries and thus it is considered to affect only the element interiors. Superscript e in (9) denotes the element under consideration. The velocity \mathbf{u}^e is a characteristic value for this element, that we take as the mean velocity over the element. For transient and iterative algorithms, this velocity is calculated using the values obtained in the last iteration of the current time step.

The parameter τ^e is defined as:

$$\tau^e = \frac{\beta^e h^e}{2|\mathbf{u}^e|} \tag{10}$$

where β^e is the upwind function and h^e the characteristic element length, that we compute as⁴:

$$\beta^e = \beta_0 \min\{(\text{Re})^e/3, 1\}, \quad h^e = \frac{|\mathbf{u}^e|}{|\mathbf{u}_0^e|} h_0, \quad (\text{Re})^e := \rho \frac{|\mathbf{u}^e| h^e}{2\mu^e}$$

with $\beta_0 = 1$ for linear elements and $1/2$ for quadratic elements. Subscript nought refers to values in the standard parent domain¹⁴. We take $h_0 = 0.7$ for triangles and 2.0 for quadrilaterals. $(\text{Re})^e$ is the cell Reynolds number and μ^e the mean viscosity over the element.

It is observed from (9) that the perturbation ζ_h only involves *the convective operator* of the Navier–Stokes equations. In this case, the discrete velocity and pressure spaces have to satisfy the BB stability condition, as for the Galerkin approach. It is also possible to introduce a perturbation involving the pressure test function, which allows to circumvent this condition and therefore to use equal-order interpolations for the velocity and the pressure⁹.

The same procedure is applied for the temperature equation, replacing the cell Reynolds number by the cell Péclet number $(\text{Pe})^e := \rho c_p |\mathbf{u}^e| h^e / 2k$, and also for the pseudo-concentration equation, now taking $\beta^e = \beta_0$.

We shall consider that the matrices and vectors in (5)–(8) account for the SUPG contributions. For further details the reader is referred to Reference 3.

Discretization in time

The generalized trapezoidal rule has been used to discretize the time derivatives of (5)–(8). Let $\alpha \in [0, 1]$ be given. For a differential equation of the form $\dot{\mathbf{x}} + \mathbf{A}(\mathbf{x})\mathbf{x} = \mathbf{f}$, \mathbf{x} being the vector of nodal unknowns and \mathbf{A} a matrix, the time discretization leads to:

$$\mathbf{x}^n + \Delta t \alpha \mathbf{A}(\mathbf{x}^n) \mathbf{x}^n = \mathbf{x}^{n-1} - \Delta t (1 - \alpha) \mathbf{A}(\mathbf{x}^{n-1}) \mathbf{x}^{n-1} + \Delta t \alpha \mathbf{f}^n + \Delta t (1 - \alpha) \mathbf{f}^{n-1}$$

where Δt is the time step size and the superscript denotes the time step. For $\alpha = 0$ this is the forward Euler scheme, which happens to be unconditionally unstable for the Navier–Stokes equations due to the zero divergence restriction. For the examples presented later, we have used $\alpha = 1$ (backward Euler), yielding an unconditionally stable and first order accurate algorithm.

Iterative techniques

We shall briefly describe now the iterative techniques employed to solve the non-linear problem (5)–(8) once the time discretization has been performed. First, let us consider the momentum equation (5). The convective term may be linearized either up to first order (Picard scheme) or up to second order (Newton–Raphson algorithm). The nonlinear terms arising from the application of the SUPG formulation are difficult to linearize up to second order. We shall

adopt the simple Picard scheme (fixed point), which also has a much larger attraction ball than the Newton–Raphson method. Also, when the problem is thermally coupled we use a block-iterative algorithm³, whose convergence rate is only linear. Therefore, there is also not much gain in using a second order linearization of the Navier–Stokes equations in this case.

Both the iterations due to the linearization of the momentum equation and the block iterative algorithm, if needed, will be dealt with in a single iterative loop, in which also the following iterative penalty method will be introduced. Let n and i denote the time step and iteration counters, respectively. The standard penalty method consists in replacing the incompressibility equation (6) by:

$$\varepsilon \mathbf{M}_p \mathbf{P}^{n,i} + \mathbf{G}^T \mathbf{U}^{n,i} = \mathbf{0} \quad (11)$$

where ε is a small positive number and \mathbf{M}_p is the Gramm matrix coming from the pressure interpolation. The artificial compressibility method would lead to

$$\varepsilon \mathbf{M}_p \mathbf{P}^{n,i} + \mathbf{G}^T \mathbf{U}^{n,i} = \varepsilon \mathbf{M}_p \mathbf{P}^{n-1} \quad (12)$$

which results from the discretization of the mass conservation equation for a slightly compressible fluid:

$$\frac{1}{c^2} \frac{\partial p}{\partial t} + \nabla \cdot \mathbf{u} = 0 \quad (13)$$

after identifying ε with $1/c^2 \Delta t$, c being the speed of sound in the fluid and Δt the time step size. To arrive at (12) from (13) the backward Euler scheme in time has to be employed.

Instead of using the standard penalty method (11) or the artificial compressibility method (12), we use the following:

$$\varepsilon \mathbf{M}_p \mathbf{P}^{n,i} + \mathbf{G}^T \mathbf{U}^{n,i} = \varepsilon \mathbf{M}_p \mathbf{P}^{n,i-1} \quad (14)$$

This method is described in detail for non-Newtonian flows and fully analyzed for the Navier–Stokes equation in Reference 32. The incompressibility restriction is iteratively approximated as the iterative procedure goes on, thus allowing to use penalty parameters much larger than using (11). This is an aspect of fundamental importance when the pseudo-concentration technique is used, since in this case the viscosity of the fluid analyzed may be several orders of magnitude larger than that of the fictitious material, and therefore, the problem is itself ill-conditioned. If very small values of ε are used, this ill-conditioning is aggravated.

FRONT SMOOTHING AND AIR RELEASE

The use of the pseudo-concentration method described above provides a basic technique to track free-surfaces of viscous incompressible flows, although several problems appear when it is implemented in a computer code. One of them is the choice of the function ψ . If we take a step function, as indicated before, numerical problems may be encountered when it is transported. It is known that small oscillations in the vicinity of sharp gradients still remain using the SUPG formulation¹⁰. These oscillations may propagate and yield to distorted front shapes, especially near corners. Since the basic idea of the method does not depend on the choice of the function ψ , it is preferable to use a smooth function instead of one with abrupt changes. The smoothing technique we employ will be discussed below. Nevertheless, we have found that if the peaks encountered when dealing with a step function are just eliminated for each time step, an accurate tracking of the front is obtained using the SUPG method.

Another problem to be considered is the evacuation of air bubbles. Since we deal with incompressible flows, air cannot shrink and air bubbles near the corners will remain if a method to evacuate them is not devised. In practice, moulds are made of porous materials, usually sand

in casting applications. Therefore, air can leave the mould without resistance. Numerically, a possible way to evacuate air is to introduce holes on the boundary and to block them when the fluid touches the wall. This method will also be explained in the following.

Smoothing of the pseudo-concentration surface

Even if the initial condition $\psi_0(\mathbf{x})$ is a smooth function, if the pseudo-concentration is maintained unmodified over several time steps it may begin to lose its smoothness and numerical problems may be encountered. Since the only important factor is the location of the critical contour that defines the front, it is possible to smooth ψ while maintaining the position of this critical contour. Following Thompson¹², this can be performed redefining the pseudo-concentration for each node of the finite element mesh according to the following expression:

$$\psi = \psi_c + \text{sgn}(\psi_0 - \psi_c)\sigma d \quad (15)$$

where ψ_0 stands for the calculated value of ψ , σ is a given constant, d is the distance from the node under consideration to the front and $\text{sgn}(\cdot)$ is the signum of the value enclosed in the brackets.

Equation (15) indicates that the smoothed pseudo-concentration is obtained adding or subtracting to the critical value a quantity proportional to the distance to the front, according to which material occupies the point (the fluid analyzed or air). The constant σ is the slope of the new pseudo-concentration surface in the direction normal to the front.

The crucial point is how to calculate the distance d from a point under consideration to the front. The method we have used for 2-D problems will now be briefly described.

Once we know the values of the pseudo-concentration for all the nodal points, it is possible to calculate the position of the points of the front located at the sides of the elements. This can be done by checking if the sign of $\psi - \psi_c$ changes when passing from a certain node of an element to the adjacent one. When this happens, the position where the value ψ_c is attained can be computed using a linear interpolation between the values of ψ at the two nodes identified and the coordinates of these two nodes. In the most common case in which only one front crosses the element, two front points which are part of the element sides will be found. Between these two points, the position of a specified number of additional front points may be calculated by interpolating the front within each element by a straight line. If more than a single front crosses the element, an even number of front points lying on the element sides will be found. The way to connect pairs of them is easily established by moving along the boundary and checking the sign of $\psi - \psi_c$.

When the process just described is finished, the front will be represented by a set of points lying on straight segments within each element. The distance d from a considered point to the front is then computed as the minimum of the distances to all these front points.

The accuracy of this method depends on the smoothness of the front (not on the pseudo-concentration), as well as on the number of front points to be interpolated within each element. Clearly, if the front presents a sharp corner within a certain element, the approximation by a straight segment will be indeed poor. Moreover, advancing in time the approximation error will add up and the final representation of the front may be completely wrong. In these cases the smoothing of the pseudo-concentration is not recommended. We have solved some problems of this kind just using a step function for ψ and without smoothing. However, when the front is smooth, this method has proved to be quite effective. In general, we have found that four or five additional front points interpolated within each element are needed when quadratic elements are used.

For the particular case of finite elements with interior nodes, such as the Q_2/P_1 or the P_2^+/P_1 (quadratic velocities enriched with bubble functions, piecewise linear pressures) pairs, this smoothing technique has an additional problem that we have observed while running some test cases. Let us consider the situation illustrated in *Figure 1* for the two-dimensional Q_2/P_1 element.

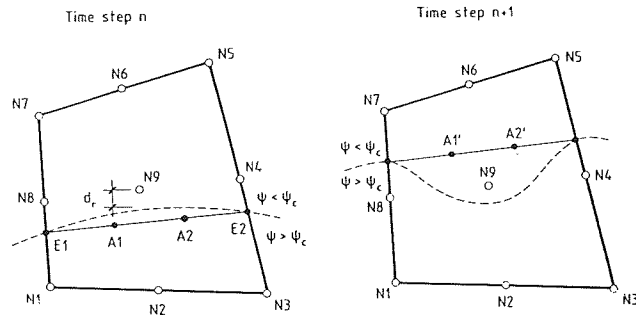


Figure 1 Formation of spurious air-bubbles for interior nodes. The dashed line denotes the critical contour ψ_c .

The nodes of the element have been denoted by $N1, N2, \dots, N9$, the front points located on the sides of the element by $E1, E2$ and the additional front points by $A1, A2$. In the situation of the picture on the left of Figure 1, application of (15) computing the distance d as explained above will lead to

$$\psi_9^n = \psi_c - \sigma \min\{\text{dist}(N9, A1), \text{dist}(N9, A2)\} < \psi_c - \sigma d_r \quad (16)$$

where d_r is the real distance from node $N9$ to the front. The inequality (16) indicates that we are underestimating the value of ψ at node $N9$. The error will be much smaller for nodes $N4$ and $N8$. After solving the transport equation for the pseudo-concentration it may happen that nodes $N4$ and $N8$ are already part of the fluid whereas node $N9$ remains in the unfilled region (see the picture on the right of Figure 1). Since the fluid front will be again approximated by a straight segment, node $N9$ may be situated at the wrong side of this. Applying again (15) we will obtain:

$$\psi_9^{n+1} = \psi_c - \sigma \min\{\text{dist}(N9, A1'), \text{dist}(N9, A2')\} < \psi_c$$

It is even possible that $\psi_9^{n+1} < \psi_9^n$. In any case, there exists the possibility that as the fluid front advances a spurious bubble around node $N9$ be left behind. We have observed this misbehaviour in practice.

The way to circumvent this problem is quite simple. Once the values of the smoothed pseudo-concentration for the nodes lying on the element sides have been calculated using (15), the value for the interior node is computed from interpolation. The serendipid interpolation (Q_2^-) is used for the biquadratic element (Q_2) and the quadratic simplicial interpolation (P_2) for the enriched simplex P_2^+ .

Air release—Introduction of holes

It has already been said that in practical problems air can leave the mould through its porous walls. Numerical models must incorporate a facility to evacuate air in order to prevent the appearance of air bubbles, especially near the corners.

The basic idea of the method to be described now is to place some holes in the walls of the mould and to block them when the fluid reaches these walls. Thus, air will be allowed to leave the mould but the fluid analyzed will not.

To motivate the basic inconvenience of this method, let us describe how boundary conditions are implemented in the computer code developed in this work. If a boundary node has a Neumann type prescription, its velocity is one of the unknowns of the problem. But if a Dirichlet condition is prescribed there, the velocity vector is known. The columns and rows corresponding to the node under consideration of the assembled matrix of the final algebraic system are not needed. The product of the columns by the velocity components of the node are moved to the

right-hand-side. The matrix of the resulting reduced system, say \mathbf{A} , will be smaller than if these columns and rows are not eliminated. Since we work with dynamic memory allocation, the dimension of matrix \mathbf{A} has to be known before starting the analysis, after reading the data of the problem. Hence, the change of a node from a Neumann boundary condition to a Dirichlet boundary condition during the analysis is not so simple as it might seem at first glance.

In order to avoid the need for changing the size of the problem, we leave the nodes located at the holes always free. When the fluid reaches them, the velocity (or perhaps only the component normal to the wall) is prescribed to zero not exactly, but through penalization.

To describe this method, let us consider a generic linear system of the form:

$$\mathbf{Ax} = \mathbf{b} \quad (17)$$

where \mathbf{x} is a vector of n unknowns. Suppose that the i th component of \mathbf{x} is to be prescribed to a value \bar{x} , i.e., $x_i = \bar{x}$. From (17) we will have that:

$$a_{ii}x_i = b_i - \sum_{j=1, j \neq i}^n a_{ij}x_j \quad (18)$$

Assume that the component a_{ii} of matrix \mathbf{A} is not zero and replace:

$$\begin{aligned} a_{ii} &\leftarrow a_{ii}(1 + \lambda) \\ b_i &\leftarrow \bar{x}a_{ii}(1 + \lambda) \end{aligned} \quad (19)$$

From (18) it follows that:

$$x_i = \bar{x} - \frac{1}{a_{ii}(1 + \lambda)} \sum_{j=1, j \neq i}^n a_{ij}x_j$$

and therefore $x_i \rightarrow \bar{x}$ as $\lambda \rightarrow \infty$.

In practice, we have observed that values of λ of order 10^6 yield a good enough approximation to the prescription to be imposed (observe that λ is dimensionless).

The way to block the holes is now clear. For a certain time step, the value of the pseudo-concentration at the point of interest is computed. If this value ψ is lower than ψ_c , $\lambda = 0$ is taken for the system analogous to (17) arising from the fully discrete and linearized Navier–Stokes equations and the redefinition (19) is not performed. Otherwise, a high value of λ is selected, taking $\bar{x} = 0$ in (19).

Consider now the transport equation for the pseudo-concentration. If for a certain time step the velocity at a node lying on the hole is left free, it may point into the mould due to suction effects. In this situation, the hole must be considered as a part of the inflow boundary Γ_{inf} and therefore the function ψ must be prescribed there. Otherwise, it may happen that values of ψ higher than ψ_c be transported into the mould, thus introducing spurious fluid. The situation is similar to what happens for the one-dimensional hyperbolic equation:

$$\frac{\partial \psi}{\partial t} + u \frac{\partial \psi}{\partial x} = 0, \quad 0 < x < 1$$

If $u > 0$ and the value of ψ at $x = 0$ is not prescribed, the solution is simply $\psi(x, t) = \psi_0(x - ut)$, where $\psi_0(x)$ is the initial condition extended by periodicity to the whole real line \mathbb{R} .

There is another way to see that if ψ is not prescribed at the nodes for which the velocity points into the mould then spurious material will be introduced. Let V_t be any control volume surrounding this node. Multiplying the equation in (4) by ψ , integrating over V_t and using the fact that \mathbf{u} is divergence-free yields:

$$\frac{d}{dt} \int_{V_t} \psi^2 d\Omega = -\frac{1}{2} \int_{\partial V_t} (\mathbf{n} \cdot \mathbf{u}) \psi^2 d\Gamma$$

Box 1 Checks for temporary free wall nodes

- IF $\psi_b^{n-1} < \psi_c$ then
 - IF $\mathbf{n} \cdot \mathbf{u} < 0$ then
 - Prescribe ψ_b^n to ψ_b^{n-1}
 - ELSE
 - Leave ψ_b^n free
 - END
 - Leave \mathbf{u} free (Neumann type condition)
- ELSE
 - Prescribe $\mathbf{u} = \mathbf{0}$
 - Leave ψ_b free

END

If ψ is not prescribed where $\mathbf{n} \cdot \mathbf{u} < 0$, the integral of ψ^2 over V_t may increase as time goes on, and this happens for any control volume V_t , that is, a spurious fluid-filled region may appear around the hole.

Having these considerations in mind, it is clear that the pseudo-concentration must be prescribed at the temporary free wall nodes where $\mathbf{n} \cdot \mathbf{u} < 0$. For a certain time step, the value of the prescription will be the value obtained in the previous one. The way to implement this is the same as for the velocities in the Navier–Stokes equations. Let ψ_b^{n-1} the value of the pseudo-concentration at the node under consideration for time step $n - 1$. Considering that the system to be solved to find ψ for time step n is (17), the redefinition (19) will be employed, with $\bar{x} = \psi_b^{n-1}$. Again, we have found that good results are obtained taking λ of order 10^6 .

The checks to be performed for temporary free boundary nodes are summarized in *Box 1*. It is understood that all the variables (pseudo-concentration and velocity) refer to a certain node and that Dirichlet boundary conditions are prescribed according to the penalty technique described here.

SOME FURTHER REMARKS

Using the pseudo-concentration method, the value of the physical properties has to be stored for each integration point of each element. Let us denote by π any of them and by π_k^e its value at the k th integration point of the e th element. To determine how to calculate it we first must know the value of the pseudo-concentration at this point, $\psi^e(\xi_k)$, which is easily calculated from the standard interpolation from the nodal values of ψ for the element. Then, the discrete counterpart of (3) is:

$$\pi_k^e = \begin{cases} \pi_{\text{fluid}}^e(\xi_k) & \text{if } \psi^e(\xi_k) \geq \psi_c \\ \pi_{\text{air}} & \text{if } \psi^e(\xi_k) < \psi_c \end{cases} \quad (20)$$

The property π for the fluid analyzed may depend on the velocity and the temperature (see examples in Reference 5). For the *air*, it may be any constant provided that the motion of the resulting fictitious fluid do not affect the motion of the *real* fluid. There is also the possibility of using the real air properties. We do not use any averaging of properties within the elements.

The final transient and iterative algorithm is given in *Box 2* (terms in italics denote logical variables, N is the total number of time steps). The basic calculations needed to track the free surface are included. The pseudo-concentration may be calculated at the beginning of the time step or at the end (staggered with respect to the Navier–Stokes equations). This last choice is considered in *Box 2*. Both options are equally valid, but one must keep in mind that if the former is chosen the front will be ‘delayed’ one time step with respect to the velocity and pressure,

Box 2 General algorithm including free-surface tracking

- Set the initial condition $\mathbf{U}^0, \mathbf{P}^0 = \mathbf{0}, \Theta^0$ and Ψ^0
- $n := 0$
- WHILE $n < N$ and (*non-stationary*) DO:
 - $n \leftarrow n + 1$
 - $i := 0$
 - WHILE (*not converged*) DO:
 - $i \leftarrow i + 1$
 - Solve the Navier–Stokes equations
 - Update the physical properties and forcing terms
 - Check convergence
 - END while (*not converged*)
 - Solve the temperature equation
 - Check the sign of $\mathbf{n} \cdot \mathbf{u}$ for the temporary wall nodes and adjust the boundary conditions for ψ (see *Box 1*)
 - Solve the pseudo-concentration equation
 - Smooth the pseudo-concentration (see (15))
 - Update the physical properties according to (20)
 - Check whether $\psi \geq \psi_c$ or $\psi < \psi_c$ for the temporary free wall nodes and adjust the boundary conditions for \mathbf{u} (see *Box 1*)
 - Check if the steady-state has been reached
- END while $n < N$ and (*non-stationary*)
- END

whereas if the second possibility is adopted the situation will be the inverse. It could also be possible to include the calculation of the pseudo-concentration within the block iterative loop. We have found that this leads to convergence problems, which are due to the fact that an integration point may belong to the fluid in a certain iteration and to the air in the next one, thus having different physical properties from iteration to iteration.

In *Box 2*, it is understood that the boundary conditions for the temporary free wall nodes are always adjusted using the penalization method described in the section entitled ‘Front Smoothing and Air Release’.

In the most common situation, the fluid front will cross an element. For some of its integration points the properties of the fluid will be used and for the others the properties of the air. Clearly, the accuracy of the integration rule will be poor for these elements, although this should not affect much the global accuracy. Also, there will be a jump in the fluxes of temperature and stresses that we have not considered. Let us denote by Γ_f^e the part of the front crossing element e . Considering for example the temperature equation, this jump (arising from the application of the divergence theorem) will be

$$\int_{\Gamma_f^e} \eta [k_{\text{fluid}} \mathbf{n} \cdot (\nabla \vartheta)_{\text{fluid}} - k_{\text{air}} \mathbf{n} \cdot (\nabla \vartheta)_{\text{air}}] d\Gamma$$

where η is the test function for the temperature. For the finite element discretization, the derivatives of ϑ within each element will be continuous, i.e., $(\nabla \vartheta)_{\text{fluid}} = (\nabla \vartheta)_{\text{air}}$, and therefore this integral will not vanish if the diffusions are different. The continuity of heat fluxes for the continuous problem implies that the bracketed term must be zero. The influence of the inclusion of the jump in the finite element problem is an aspect that deserves greater attention.

Let us finally mention that the iterative penalty method defined by (14) has proved to be a fundamental ingredient for the success of the pseudo-concentration technique. In practical situations, especially for highly viscous flows, the viscosity of the fictitious material will be several orders of magnitude smaller than that of the fluid analyzed. Even if the exact value for the air

is not used, it must be between 3 and 5 orders of magnitude smaller. Hence, choosing *a priori* a penalty parameter for the classical penalty method will yield unavoidably a poor approximation to the incompressibility constraint or to ill-conditioning. This is aggravated by the fact that contiguous elements may have stiffness matrices of an order of magnitude completely different. We have observed from several numerical experiments that if ε is taken as $\varepsilon = 10^{-n} \mu_{\text{fluid}}^{-1}$ (assuming the fluid viscosity to be constant) and $\mu_{\text{air}} = 10^{-3} \mu_{\text{fluid}}$, ill-conditioning is observed for values of n as small as 3 (we have used the check proposed in Reference 14, Chapter 15, for ill-conditioning).

NUMERICAL EXAMPLE

We shall now present some results for the numerical simulation of the filling of the mould shown in *Figure 2*. The geometry and experimental results for this problem have been provided by *Renault Automobiles*. The experiments have been carried out using Gallium, a metal well suited to experimentation because it has a low fusion point (30°C) and, therefore, it is easy to use and recover it in the laboratory, once the experiments are finished. Moreover, its properties are close enough to those of the aluminium and other metals used in casting applications.

The molten metal enters through the left gate shown in *Figure 2* with a horizontal velocity of 0.31 m/s. The vertical velocity is accommodated to the slope of the top wall of the entering gate. The physical properties of the molten Gallium at 55°C (all in SI units) are $\rho = 5.9 \times 10^3$ (density), $\mu = 1.9 \times 10^{-3}$ (dynamical viscosity), $k = 30.4$ (thermal conduction coefficient) and $c_p = 250$ (specific heat at constant pressure). Thus, the Reynolds number based on the velocity that enters the cavity (0.62) and its longitudinal length (0.1) is $Re = 1.93 \times 10^5$. The flow is clearly turbulent for such a high Reynolds number and it is impossible to simulate it with a laminar model such as ours. The physical properties of air are $\rho = 1.2$, $\mu = 1.8 \times 10^{-5}$, $c_p = 1005$ and $k = 0.0256$. In order to reproduce the relative importance of all the physical effects, we have used the real properties of the Gallium and the air except for the dynamical viscosity, which

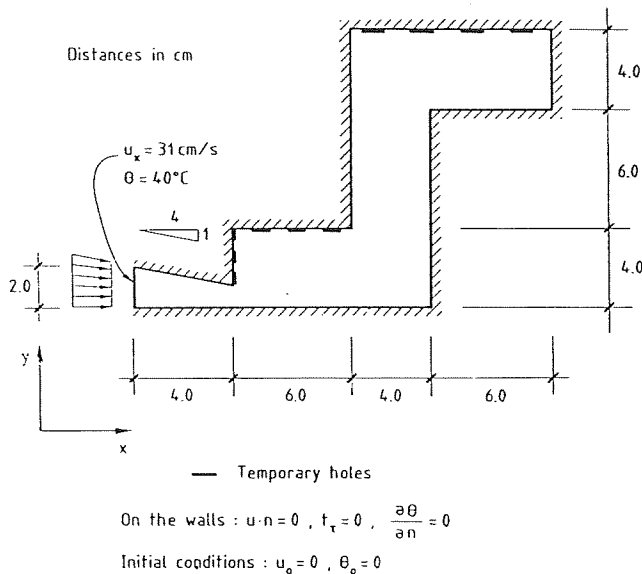


Figure 2 Geometry and boundary conditions

has been taken 10^n times higher for both the Gallium and the air. Results are qualitatively similar for $n = 3$ and $n = 2$ (the value used here). We failed to obtain a converged solution for lower values of this exponent.

The boundary conditions for this problem are normal velocities at the walls and zero tangential stresses, i.e., no friction with the walls is considered. The fluid is assumed to be initially at the entrance of the left gate. A thermally uncoupled flow model is adopted. Therefore, it is possible to deal with relative temperatures. The temperature of the Gallium has been assumed to be 40°C higher than that of the air. The walls of the mould have been assumed to be adiabatic, although we know that this is not realistic.

The finite element mesh designed for this problem is shown in *Figure 3*. It consists of 548 Q_2/P_1 elements and 2351 nodal points. The iterative penalty method has been employed, using a penalty parameter $\varepsilon = 10^{-4}$. The backward Euler scheme has been used to advance in time for the three transient problems to be solved (velocity-pressure, temperature and pseudo-concentration). The smoothing technique described in Section 4 has been used, with $\sigma = 1$ and five additional points within each element to compute the distance d (see (15)). Within each time step, of size $\Delta t = 0.01$, the advection of the pseudo-concentration has been solved first and then iterations have been carried out (between three and four) to obtain a converged solution of the Navier-Stokes equations (with a tolerance 0.1%). Finally, the temperature equation has been solved.

In order to allow the air evacuation, some holes have been introduced on the walls of the mould. They are schematically shown in *Figure 2* (three or four nodes of the finite element discretization correspond to each hole). The parameter λ to block them when the Gallium touches the wall has been taken as $\lambda = 10^6$.

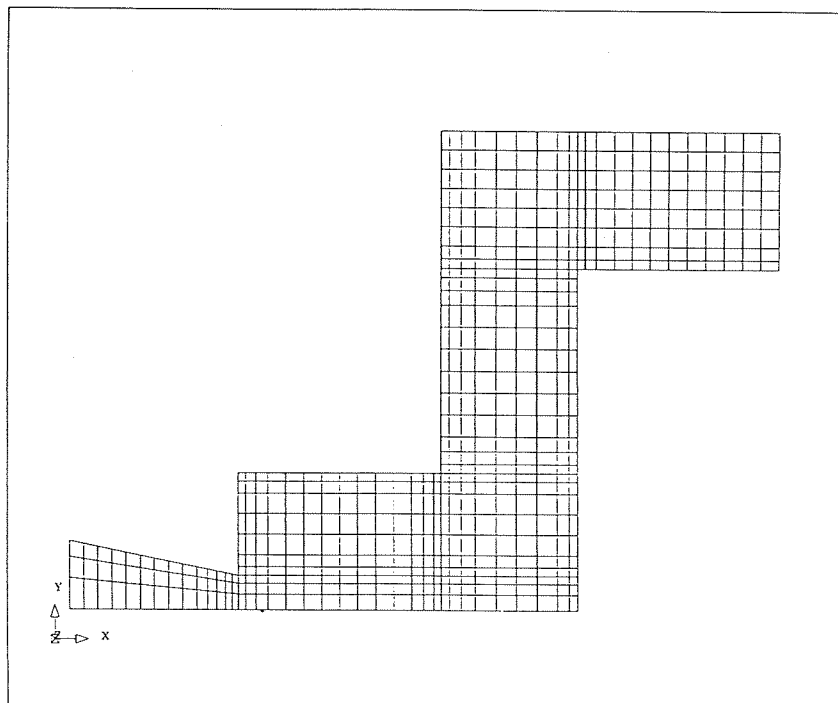


Figure 3 Finite element mesh (548 Q_2/P_1 elements, 2351 nodal points)

The position of the fluid front at different times is depicted in *Figures 4–7*. It is observed how several air bubbles appear in the Gallium. This fact is also observed in the experimental results, with which the numerical simulation shows a good qualitative agreement. These experimental results are shown in the colour pictures for $t = 0.2, 0.6, 1.2, 1.4, 1.6$ and 1.8 , approximately. The differences should be attributed to the different Reynolds number of the numerical calculation. Air bubbles disappear as time goes on due to the artificial effect of the smoothing technique. Observe from *Figure 1* that the interpolation of the front by a straight segment within each element will advance or delay artificially the front depending on its curvature. Physically, air bubbles disappear because air can escape through the porous lateral walls of the sand mould.

Figures 8 and 9 show the position of the fluid front, the streamline pattern, the pressure contours and the temperature contours at different times. From the streamline plots, it is observed how air enters or leaves the mould through the holes, as well as the creation of vortices due to the transmission of shear stresses. From the pressure plots it is seen that pressure gradients are rapidly dissipated in the air region. This indicates that the motion of air does not influence much that of the Gallium. Iso-temperature curves show how heat is basically transported through convection. Conduction transport is only apparent in regions occupied by Gallium that has first entered the cavity. It is remarkable to note the high temperature gradients that the numerical method is able to capture at the interface between hot Gallium and cold air.

Referring now to some computational aspects of the calculation, the behaviour of the iterative penalty method has been found to be very effective. The convergence history and the evolution of the norm of the incompressibility constraint for time step number 77 are shown in *Figure 10*. It is observed that this norm decreases almost three orders of magnitude in four iterations. This decrease is even more accentuated for the first time steps (not shown). Starting from a value of order 10^{-7} , a final value of order 10^{-11} is obtained in four iterations.

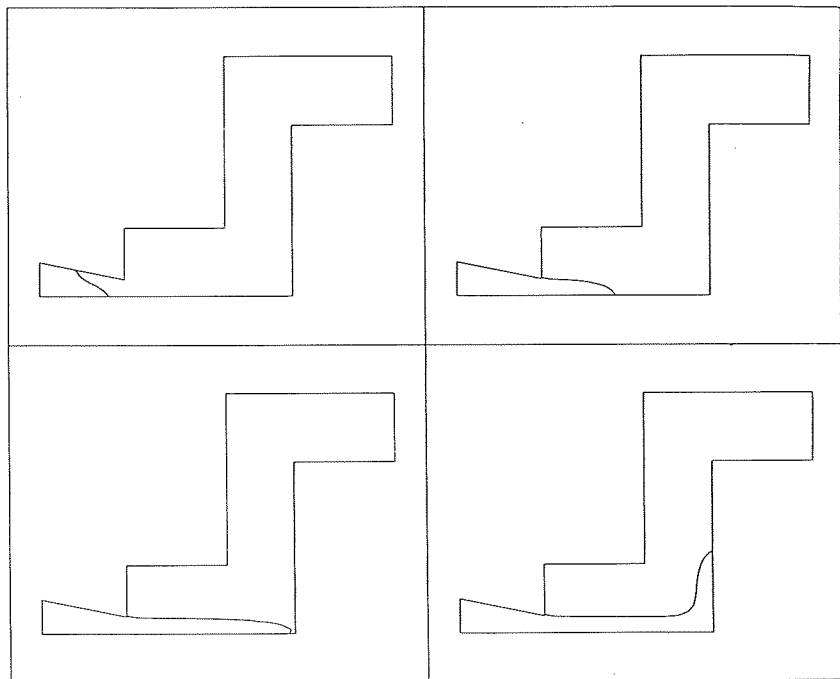


Figure 4 Positions of the fluid front for $t = 0.1, 0.2, 0.3$ and 0.4

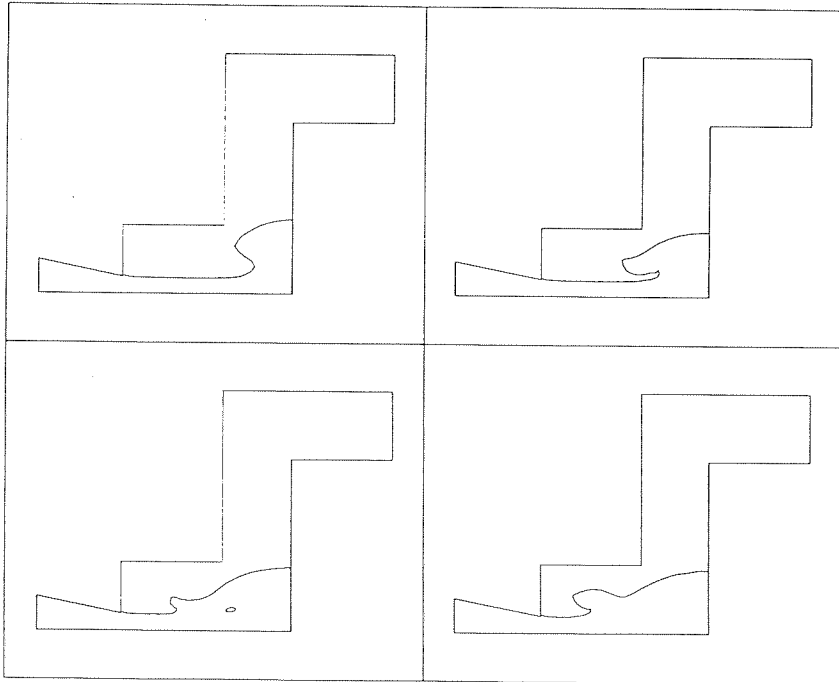


Figure 5 Positions of the fluid front for $t = 0.50, 0.55, 0.60$ and 0.65

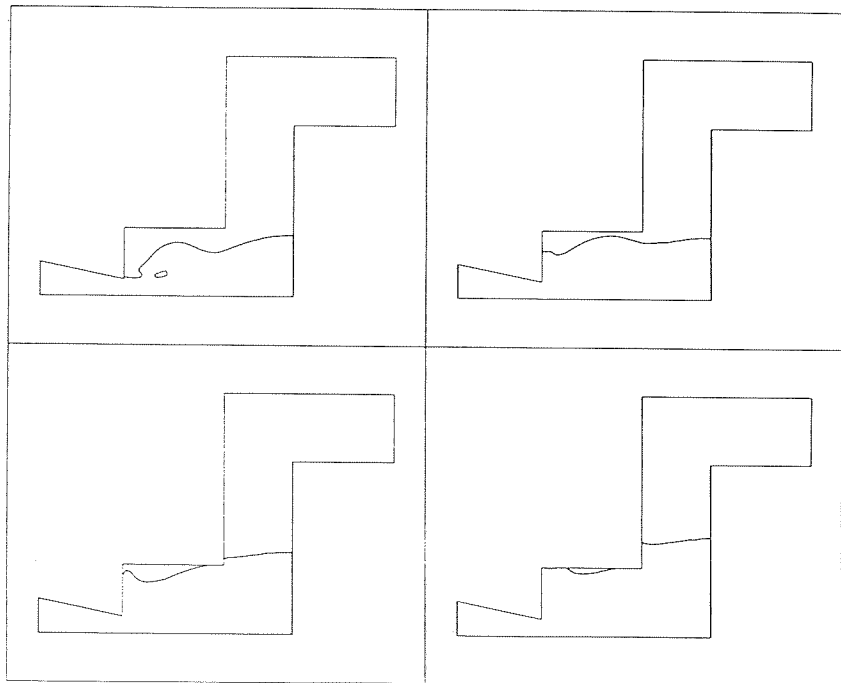


Figure 6 Positions of the fluid front for $t = 0.7, 0.8, 0.9$ and 1.0

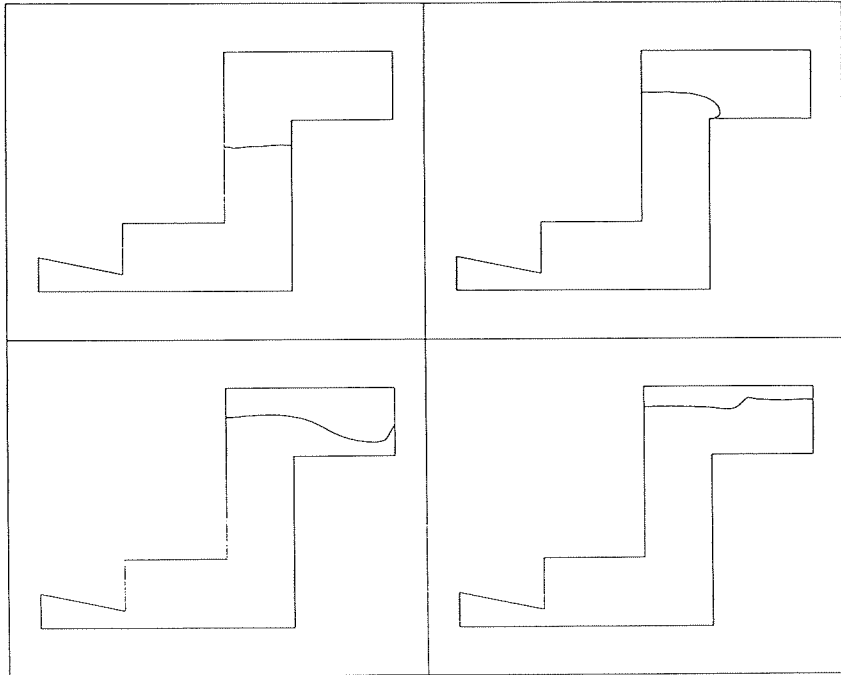


Figure 7 Positions of the fluid front for $t = 1.2, 1.4, 1.6$ and 1.8

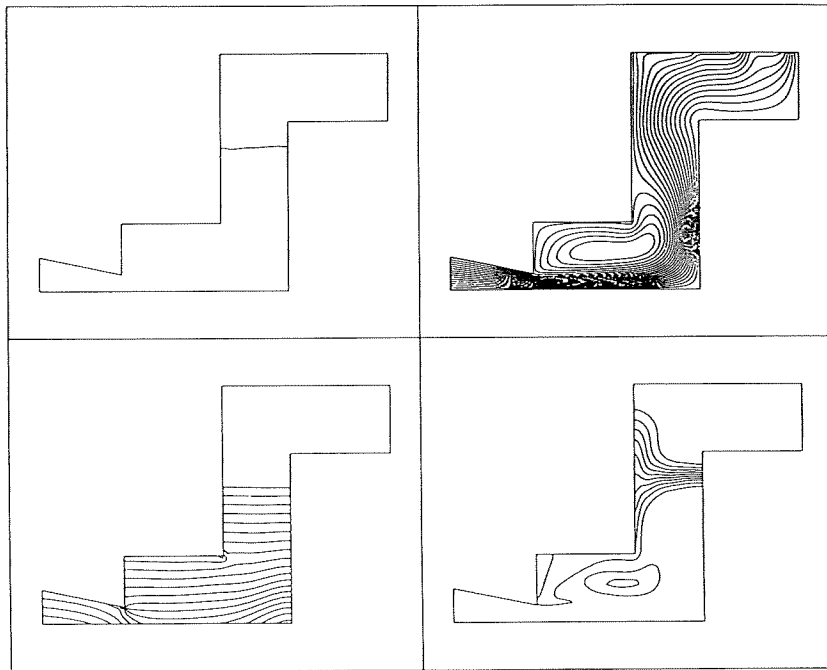


Figure 8 Some relevant physical results at $t = 1.2$ (1): Position of the front; (2) streamlines; (3): pressure contours (max = 5.99 Mpa, min = -1.33×10^{-2} Mpa, pressure increment between contours = 0.27 Mpa); (4): temperature contours (max = 40.1°C, min = 0.0°C, temperature increment between contours = 3.6°C)

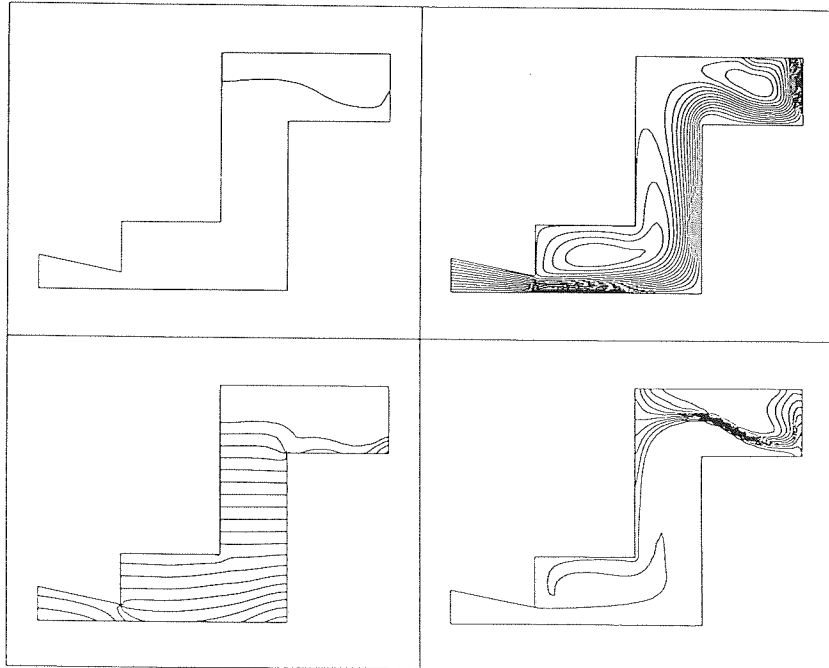


Figure 9 Some relevant physical results at $t = 1.6$. (1): Position of the front; (2): streamlines; (3): pressure contours (max = 8.46 Mpa, min = -8.11×10^{-2} Mpa, pressure increment between contours = 0.385 Mpa); (4): temperature contours (max = 40.2°C, min = 0.056°C, temperature increment between contours = 3.5°C)

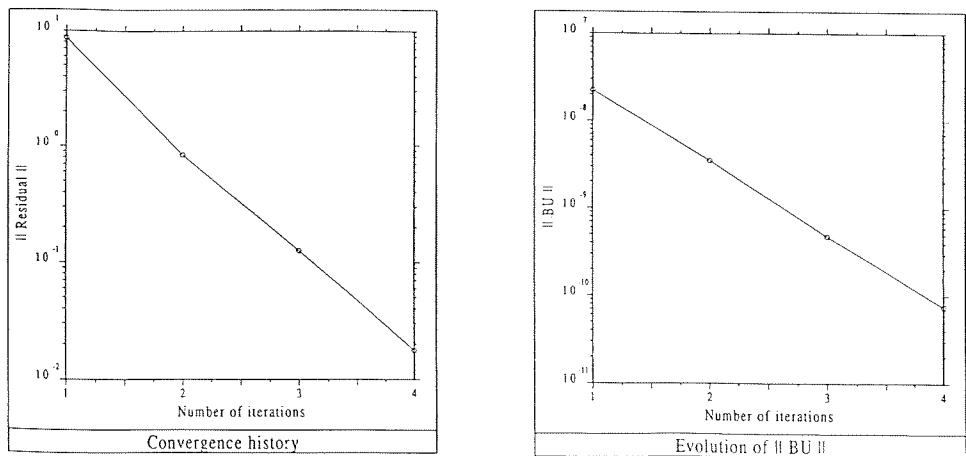


Figure 10 Convergence history and evolution of the norm of the incompressibility constraint for time step number 77

Most of the computational cost of the simulation is due to the solution of the Navier–Stokes equations. The CPU time per iteration needed on a CONVEX-C320 computer has been 24.27 seconds (54.96% for the formation of the element matrices, 44.96% for the solution of the linear system). The pseudo-concentration and the temperature equations are solved only once per time step. The CPU time needed has been 5.03 (11.54% for the element matrices, 52.98% for the

linear system, 35.48% for the smoothing and updating of physical properties) and 3.05 seconds (24.83% for the element matrices, 75.16% for the linear system), respectively.

CONCLUSION

We have described in this paper some numerical techniques to solve the incompressible Navier–Stokes equations in combination with the method of pseudo-concentrations to track free surfaces. The crucial ingredients of the formulation are the iterative penalty method, to avoid the need for using very small penalty parameters, and the SUPG formulation to deal with convection dominated problems. Both strategies have been shown to be very effective for the practical problem presented here. Moreover, we have also considered some problems related to the application of the pseudo-concentration technique. In particular, we have described a method to compute the distance from a node to the fluid front and a numerical strategy to allow the evacuation of air from the mould has been proposed.

From the numerical example presented it may be concluded that the numerical techniques introduced here provide an effective method for tracking free surfaces with complicated shapes. There are, of course, several limitations, mainly due to the difficulty to act upon the interface air-fluid (boundary conditions, surface tension), as well as some approximations inherent to the use of discontinuous physical properties. Nevertheless, the simplicity of the method and the good performance shown in practical problems make it a valuable tool, at least for laminar flows. In most casting applications the flow is however turbulent. We plan to implement a turbulence model in a near future using the basic numerical ingredients presented in this work.

ACKNOWLEDGEMENT

This research has been supported by BRITE-EURAM contract No. BREU-CT91-0443. The data for the test problem presented in this paper and the experimental results have been provided by P. Le Roy and P. Manigot from *Renault Automobiles* in the context of this project. This support is gratefully acknowledged.

REFERENCES

- 1 Antúnez, H. J. and Idelhson, S. R. Using pseudo-concentrations in the analysis of transient forming processes, *Eng. Computations*, **9**, 547–559 (1992)
- 2 Brooks, A. N. and Hughes, T. J. R. Streamline upwind/Petrov–Galerkin formulations for convective dominated flows with particular emphasis on the incompressible Navier–Stokes equations, *Comput. Meths. Appl. Mech. Eng.*, **32**, 199–259 (1982)
- 3 Codina, R. *A Finite Element Model for Incompressible Flow Problems*, Doctoral Thesis, Universitat Politècnica de Catalunya (1992)
- 4 Codina, R., Oñate, E. and Cervera, M. The intrinsic time for the SUPG formulation using quadratic elements, *Comput. Meths. Appl. Mech. Eng.*, **94**, 239–262 (1992)
- 5 Codina, R., Schäfer, U., Oñate, E., Cervera, M. and Soto, O. A finite element model to track free surfaces of viscous incompressible flows, *Int. Conf. Num. Meth. in Eng. and Applied Sciences*, Concepción, Chile (1992)
- 6 Dhatt, G., Gao, D. M. and Ben Cheikh, A. A finite element simulation of metal flow in moulds, *Int. J. Numer. Meth. Eng.*, **30**, 821–831 (1990)
- 7 Dvorkin, E. and Petöcz, E. G. On the modelling of 2D metal forming processes using the flow formulation and the pseudo-concentration technique, *COMPLAS III. Proc. 3rd Int. Conf. Comput. Plasticity*, Spain, Pineridge Press/CIMNE (1992)
- 8 Hirt, C. W. and Nichols, B. D. Volume of fluid (VOF) method for the dynamics of free boundaries, *J. Comput. Phys.*, **39**, 210–225 (1981)
- 9 Hughes, T. J. R., Franca, L. P. and Balestra, M. A new finite element formulation for computational fluid dynamics: V. Circumventing the Babuška–Brezzi condition: a stable Petrov–Galerkin formulation for the Stokes problem accommodating equal-order interpolations, *Comput. Meths. Appl. Mech. Eng.*, **59**, 85–99 (1986)

- 10 Hughes, T. J. R., Mallet, M. and Mizukami, A. A new finite element formulation for computational fluid dynamics: II. Beyond SUPG, *Comput. Meths. Appl. Mech. Eng.*, **54**, 341–355 (1986)
- 11 Lewis, R. W., Usmani, A. S. and Cross, J. T. Finite element modelling of mould filling, *Finite Elements in the 90s* (Eds. E. Oñate, J. Periaux and A. Samuelson), Springer-Verlag/CIMNE (1991)
- 12 Thompson, E. Use of pseudo-concentrations to follow creeping viscous flows during transient analysis, *Int. J. Numer. Meth. Fluids*, **6**, 749–761 (1986)
- 13 Thompson, E. and Smelser, R. E. Transient analysis of forging operations by the pseudo-concentration method, *Int. J. Numer. Meth. Eng.*, **25**, 177–189 (1988)
- 14 Zienkiewicz, O. C. and Taylor, R. L. *The Finite Element Method*, Fourth Edition, vol. 1, McGraw-Hill (1989)

